IOPscience iopscience.iop.org

Home Search Collections Journals About Contact us My IOPscience

Mechanical properties of polyelectrolyte multilayer microcapsules

This article has been downloaded from IOPscience. Please scroll down to see the full text article.

2004 J. Phys.: Condens. Matter 16 R1105

(http://iopscience.iop.org/0953-8984/16/32/R01)

View the table of contents for this issue, or go to the journal homepage for more

Download details:
IP Address: 129.252.86.83
The article was downloaded on 27/05/2010 at 16:39

Please note that terms and conditions apply.

INSTITUTE OF PHYSICS PUBLISHING JOURNAL OF PHYSICS: CONDENSED MATTER

J. Phys.: Condens. Matter **16** (2004) R1105–R1134 PII: S0953-8984(04)65375-6

TOPICAL REVIEW

Mechanical properties of polyelectrolyte multilayer microcapsules

Olga I Vinogradova

Max Planck Institute for Polymer Research, Ackermannweg 10, 55128 Mainz, Germany
and
Laboratory of Physical Chemistry of Modified Surfaces, Institute of Physical Chemistry, Russian Academy of Sciences, 31 Leninsky Prospect, 119991 Moscow, Russia

E-mail: vinograd@mpip-mainz.mpg.de

Received 19 April 2004
Published 30 July 2004
Online at stacks.iop.org/JPhysCM/16/R1105
doi:10.1088/0953-8984/16/32/R01

Abstract

Polyelectrolyte multilayer microcapsules were recently suggested as a new type of nanoengineered microstructures and are potentially important in many areas of science and technology. The present review focuses on the mechanics of these microstructures, emphasizing novel experimental approaches and the main experimental observations. Methods based on confocal and atomic force microscopy—osmotic buckling, osmotic swelling, and compression experiments—are detailed. Also covered is the preparation of multilayer microcapsules and various encapsulation techniques. A discussion of the theoretical models suggested is given. Special emphasis is given to the analysis of experimental data. This covers regimes of deformations, the roles of elasticity and permeability in determining the capsule stiffness, the effects of ageing, molecular weight, pH, salt concentration, and organic solvent on the multilayer shell properties, a contribution from encapsulated (charged and neutral) polymers, and more.

(Some figures in this article are in colour only in the electronic version)

Contents

 © 2004 IOP Publishing Ltd Printed in the UK

1. Introduction

Recently there has been much interest in studying polyelectrolyte multilayer microcapsules [1]. These capsules are made by layer-by-layer (LbL) adsorption [2–4] of oppositely charged polyelectrolytes onto charged colloidal particles with subsequent removal of the template core [5] and can be filled by various macromolecules and nanoparticles. Polyelectrolyte microcapsules are important for a variety of potential applications such as drug delivery, catalysis, and biotechnology. At a more fundamental level, they represent a convenient system in which to study physical properties of polyelectrolyte multilayer films and polymers in confined geometry. The shell of such a microcapsule is nothing more than a free standing multilayer film. The free thin film configuration allows one to study properties not accessible in the bulk or in the supported films. Being a charged semipermeable membrane, such a shell allows rich osmotic and electrostatic equilibria for encapsulated polyelectrolytes, which makes polyelectrolyte microcapsules essentially different from all other systems studied before. In view of this, by studying such microcapsules, one might gain a better understanding of polyelectrolytes in general.

Mechanical properties are among the most important physical properties of free standing multilayer films. They define the deformation and rupture of the capsule shell under an external load, which is important for instance for ensuring protection and/or release of encapsulated materials in the delivery systems [6]. This can also help us to understand the principles underlying the mechanical behaviour of living cells. For example, elastic properties of the capsule shell can be used as an input to models of penetration of particular viruses into the biological cell [7]. Ironically, the mechanical properties remained almost certainly the least understood physical properties of the free standing (and, in fact, even supported [3]) multilayers. Little is known about the mechanical behaviour of more complex composite systems containing encapsulated materials. In recent years, however, experiments were performed in several laboratories on a variety of polyelectrolyte microcapsules. There was some variability and certain contradictions in the details of measurements and a compelling model for fitting the experimental data was lacking.

The subject of this review has thus a small, but rapidly growing literature. It would be inappropriate to attempt a comprehensive review here, or to derive some general conclusions from still limited experimental data. Instead, we would like to draw attention to recent

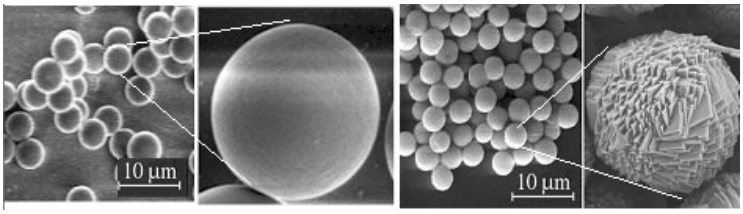

Figure 1. Electron micrographs of MF (left) and $MnCO_3$ (right) particles.

experimental observations and to provide a critical insight into the situation in this area of research. We do hope that our review will stimulate further accurate quantitative study of the mechanical and other relevant properties of polyelectrolyte multilayer microcapsules.

Our discussion does not include the range of experimental methods that have been developed previously for investigating the mechanical properties of the cells, liposomes, vesicles, and other types of microcapsules, including micropipette aspiration, poking, fluid shear, and various modifications of compression and osmotic bursting experiments [8–12]. Although some of these techniques and definitely their principles could probably be used (and, in fact, have been used [13]) for studying multilayer microcapsules, they have mostly been developed for objects at least one or two orders of magnitude larger with much thicker shells, which are, as a result, considerably stiffer. Therefore, their sensitivity is often not enough for exploring multilayer microcapsules, which are of diameter a few micrometres only, with the shell thickness of the order of 10 or 20 nm. This is not to say that they would remain invisible with the optical techniques applied previously. Therefore, in the present review the emphasis will be only on new methods, which have been developed in connection to the problems of studying the mechanical properties of polyelectrolyte microcapsules. Essentially, these methods manifest the fast development of atomic force and confocal microscopy, which dramatically increased the possibilities and accuracy of micromechanical and nanomechanical experiments.

2. Systems

To begin with, it would be appropriate to characterize the systems studied in experiments on microcapsule mechanics. Two kinds of multilayer microcapsules, namely 'hollow' (i.e. a multilayer shell filled with water or electrolyte solution) and 'filled' (i.e. a microcomposite, representing a multilayer shell with high molecular weight polymer or another material inside) have been used previously and are briefly described below. More details about the situation to 2000 are given in an earlier comprehensive review [14].

2.1. 'Hollow' capsules

2.1.1. Templates. The technology of 'hollow' capsule preparation on various templates (see figure 1) is well developed. The original technology of hollow capsule fabrication was based on the use of weakly cross-linked melamine formaldehyde (MF) templates [1, 5]. The advantage of these particles is that their suspension can easily be made monodisperse (the typical radii r_0 are normally confined in the range from 1.8 ± 0.1 to 2.5 ± 0.1 μm) and can become soluble at very mild conditions (pH 1–2). The majority of studies were carried out with such particles. However, some recent research [15] has revealed that the MF oligomers may be partly attached to the shell after MF template decomposition, which could affect the physical

Table 1. Templates used to assemble the capsules for mechanical experiments.

Template	Type	Radius (μm)	Solvent
MF [17, 22–25, 42]	Monodisperse	1.8–2.5	HCl, pH 1–2
PLA [17]	Polydisperse	2–8	1:1 mixture of acetone and (1-methyl-2-pyrrolindinone) acid
$MnCO_3$ [21, 23]	Monodisperse	2	HCl, pH 1–2
PS [26]	Monodisperse	5–10	THF

Table 2. Polyelectrolytes used to assemble the capsules for mechanical experiments.

Polyelectrolyte	Type	Mw (g mol^{-1})
PSS	Polyanion	5×10^4–1×10^6
PAH	Polycation	1.5×10^4–7×10^4
PEI	Polycation	3×10^4
PDADMAC	Polycation	2×10^5–3.5×10^5

properties of the shells. Another disadvantage is the impossibility of producing soluble MF templates of radius larger than 3 μm. The search for proper decomposable colloidal particles appropriate for polyelectrolyte shell assembly led to the exploration of other templates, such as biological cells [13], poly-lactic/glycolic acid (PLA, PLGA) particles [16, 17], weakly cross-linked polystyrene (PS) particles [18], silicon oxide and carbonate ($MnCO_3$, $CaCO_3$, $CdCO_3$) particles [19–21]. Among them, only carbonate particles become soluble at low pH. Unfortunately, the current technology only allows us to prepare monodisperse suspensions of carbonate spheres of relatively small radius (below 2 ± 0.1 μm). The dissolution of large (of the order of 10 μm) PS and PLA latex particles requires organic solvents and/or organic acids, which might modify the properties of the shells. The information about the templates used in experiments on capsule mechanics is summarized in table 1.

For the sake of brevity, the microcapsules are referred to below as MF, PLA, PS, and $MnCO_3$, depending on the templates used for their preparation.

2.1.2. Shell-forming polyelectrolytes. The driving force for multilayer formation is the electrostatic attraction between the oppositely charged species, resulting in overcharging of the films after deposition of each layer. Therefore, many kinds of charged molecules and nano-objects seem to be suitable for shell formation. Despite this, only polyelectrolytes have been employed. The majority of such studies, including those of mechanical properties [22–25], have been performed with alternating poly(sodium) styrene sulfonate (PSS) and poly(allylamine) hydrochloride (PAH). These multilayers are stable in various chemical environments. Their thickness is known to grow linearly with the number of deposited bilayers, so they represent a convenient system for investigation. Finally, such shells in normal conditions are permeable to small ions and low molecular weight solvents, but impermeable to polymer molecules. Beside PSS/PAH shells, shells with poly(ethylene imine) (PEI) [26] and poly(diallyldimethyl ammonium) chloride (PDADMAC) [27] as the polycation have been used. The information about the polyelectrolytes used is summarized in table 2.

2.1.3. Preparation. The capsules (see figure 2) are produced according to a method [5, 14, 16, 18] based on LbL assembly of several bilayers of alternating polyanions and polycations. In typical technology, the polyelectrolyte deposition is performed at 0.5–1 mol l^{-1}

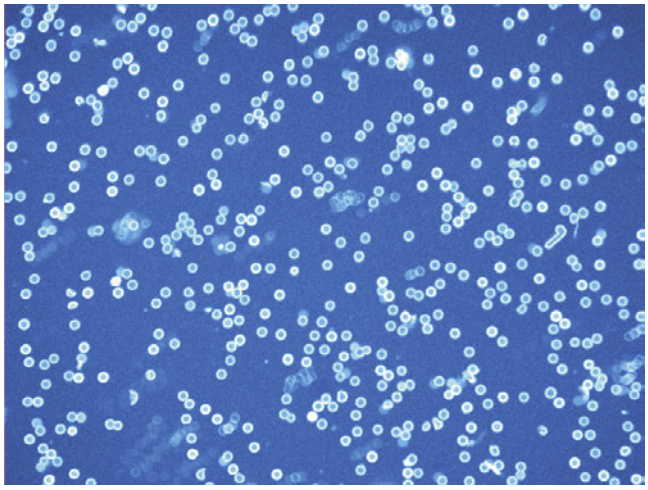

Figure 2. Confocal micrographs of the 'hollow' capsules ($r_0 \approx 2$ μm) made on the MF template.

NaCl in order to increase the bilayer thickness [3, 28–32]. Variation of the shell thickness can be achieved by two methods. First, one can vary the number of bilayers deposited on the templates. Second, one can dissolve the template particles after the deposition of the fourth bilayer, and then deposit several additional bilayers to tune the final shell thickness [17]. In the experiments reported, the numbers of bilayers varied in the range from four to ten. The value of h is normally then calculated as the product of the number of bilayers in the shell and the thickness of one bilayer. The values reported for the thickness of a PSS/PAH bilayer assembled in standard conditions vary in the range ≈3–5 nm [5, 33, 34]. In the estimates of Young's modulus the average value of 4 nm was usually used.

2.2. 'Filled' capsules

The 'filled' capsules can be prepared by a variety of methods. One approach is based on controlled precipitation [37], i.e. by assembly of the inner layer of polyelectrolyte shell by means of multivalent ions, with the subsequent extraction of these ions and polymer release into the capsule interior. The 'filled' capsules can also be made from 'hollow' ones by regulating their permeability [25, 35, 36] for a high molecular weight polymer by decreasing the pH [20, 35, 42], changing the salt concentration [43], or adding an organic solvent [25, 36]. Another method [40] involves synthesis in the capsule interior.

2.2.1. Encapsulation by permeability control. This technique is used to encapsulate neutral polymers and polyelectrolyte solutions of relatively low concentration [23, 25, 35, 36].

Although in the standard situation polyelectrolyte multilayer shells are impermeable to high molecular weight compounds, the permeability can be changed in response to the variation of physico-chemical conditions. This led to the idea of this method of encapsulation [35, 36].

In this technique, the encapsulation of polymer includes several steps (figure 3). The original 'hollow' capsules (figure 3(a)) are exposed to a low pH solution [35] or organic solvent/water mixture [25, 36] to make the polyelectrolyte multilayer permeable to high molecular weight polymer, and the neutral or charged polymer molecules are then added to the mixture. The permeable state of the capsule shell allows the polymers to penetrate inside (figure 3(b)). After the encapsulation the low pH solution or the mixture is diluted with water to return the multilayer shells to an impermeable state (figure 3(c)). After washing in pure

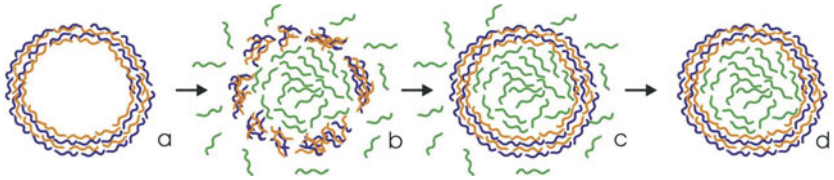

Figure 3. Encapsulation by permeability control. Reprinted with permission from [23]. Copyright (2004) American Chemical Society.

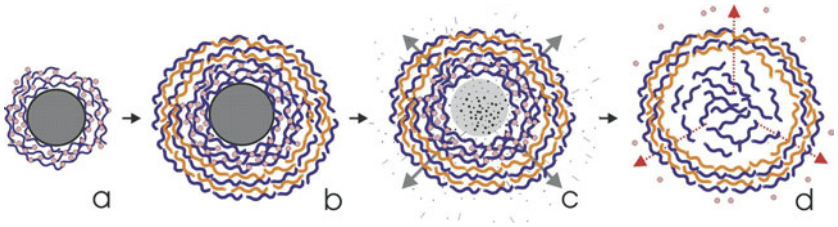

Figure 4. Encapsulation by precipitation of complexes. Reprinted with permission from [23]. Copyright (2004) American Chemical Society.

water the capsules contain encapsulated polymer solution (figure 3(d)). With such a method, the concentration of encapsulated neutral polymer or polyelectrolyte (before microcapsule swelling) is approximately equal to the final concentration in the bulk.

The apparent disadvantage of this method is the impossibility of encapsulating polyelectrolyte solutions of high concentration due to collapse/buckling of the 'hollow' capsules due to the osmotic pressure difference. Indeed, the original technology was only used for encapsulation of neutral polymers [25, 35, 36]. The solution of this problem was suggested in [23], where the concentration of bulk polyelectrolyte was increased gradually.

2.2.2. Encapsulation by precipitation of complexes. This method is normally used to encapsulate polyelectrolyte solutions of high concentration [21, 23, 24, 37, 39].

The preparation of 'filled' capsules of this type also consists of several steps (figure 4). The first step (figure 4(a)) is surface controlled precipitation of strong polyanion (by complex formation with multivalent metal Me^{3+} (Y^{3+}, Tb^{3+})) ions on the surface of a colloidal template [24, 37]. By varying the number of precipitated layers it is possible to tune the surface density for adsorbed layers, and, therefore, the number of polyanion molecules precipitated on colloidal particles. One can prepare samples with the required number of layers of adsorbed polyelectrolyte, which should lead to the required surface density, ρ (normally of the order of 10^{-5}–10^{-4} mol m^{-2}). As a result, capsules normally contain up to a few pg of polyelectrolyte, depending on the template size and number of assembled layers. With such a method, the concentration of encapsulated polyelectrolyte is approximately equal to $c = 3\rho/r_0$. The template particles are then dissolved in the appropriate solvent, which leads to the formation of 'double-shell' structured capsules (figure 4(c)). The inner shell formed by the polyanion/Me^{3+} complex is not stable and was decomposed either by metal ion complex agents (for example, EDTA) or in salt solution. Metal ions are gradually expelled out of the outer stable shell formed by alternating polyelectrolytes while inner polyanion molecules are released into the capsule interior (figure 4(d)). The same method was also successfully applied to encapsulate polycations (by complex formation with citrate) [38].

3. Experimental methods

The determination of mechanical properties of polyelectrolyte microcapsules is a difficult task due to the small size, molecularly thin shell, necessity of avoiding exposure to air, and, sometimes, fragility. For obvious reasons, it is very difficult to fix the capsules at the solid surface.

There have been several recent attempts to study the mechanical behaviour of polyelectrolyte microcapsules, and different techniques have been proposed for measuring the response of capsules to external forces. Our aim in this section is to achieve a qualitative understanding of the main principles of novel experimental approaches—namely, how the properties of the shells can be used to design an appropriate experiment, which parameters can be varied and why, and what kinds of advantages/limitations of different approaches can be expected.

3.1. Osmotically induced buckling of capsules

The first method involves observing osmotically induced buckling of capsules immersed in a polyelectrolyte solution [22, 27]. The key idea of this experiment can thus be formulated as follows. Since high molecular weight polymers cannot diffuse into the capsule interior [47], the osmotic pressure in the bulk is larger than that inside the capsule. Then the solvent is squeezed out provided that the elastic restoring forces do not compensate the pressure difference. As a result, the multilayer shell bends and a cup-like (or more complex) shape is formed. To study the capsule elasticity by this method it is necessary to prepare 'hollow' capsules of various radii r_0 and shell thicknesses h and to study the capsule shape at various concentrations of outer polyelectrolyte solutions.

Such measurements can be performed using a high resolution confocal microscopy (normally, a confocal laser scanning unit in combination with an inverted microscope equipped with a high resolution objective).

3.2. Osmotically induced swelling of capsules

The second method of evaluation of Young's modulus of the multilayer was suggested in [23]. The idea of the method is based on the earlier established experimental facts that the 'filled' capsules swell due to excess osmotic pressure of the inner solution [24, 37, 40]. At least three factors have made such experiments very attractive:

- The osmotic pressure of polyelectrolyte solutions is the sum of polymer and counter-ion contributions. However, in some situations the latter might exceed the osmotic pressure due to the polymer itself by several orders of magnitude [44–46], which considerably simplifies the analysis. The same remarks, in fact, apply to the osmotic buckling approach.
- The same (semi)permeability arguments as for an osmotic buckling experiment (now on timescales larger than the characteristic diffusion time) suggest that the solvent diffuses into the capsule until the elastic force of the stretched shell balances the osmotic pressure.
- Swelling means a pure deformation in stretching, not complicated by the bending effects.

To determine the Young's modulus, one can prepare the capsules on templates of different radii r_0 and with different concentrations c and shell thicknesses h, then measure the equilibrium size r of the swollen capsules and fit the experimental data to the appropriate theoretical expression.

This method often requires the encapsulation of fluorescently labelled polyelectrolytes, which can be synthesized according to the method of [40] and its modifications [23, 41].

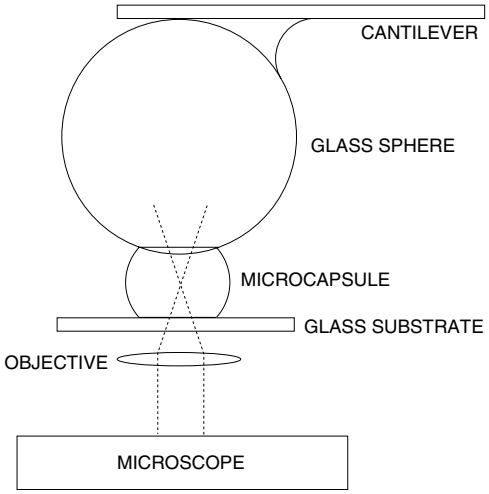

Figure 5. A schematic diagram of the AFM force experiment. Adapted from [24].

To scan the capsule shape and to measure the concentration of polyelectrolyte inside the capsules, confocal microscopy should be employed. More details about the experiments can be found in [23, 41].

The diameter of the swollen capsules can be determined with an accuracy of 0.2 μm at best, which is determined by the excitation wavelength and the steps in the confocal scanning.

3.3. Measurements of force versus deformation curves using AFM

The third approach involves measuring the deformation of microcapsules under an applied load using atomic force microscopy (AFM) [17, 21, 24–26, 42]. Forces between surfaces have been intensively studied with an AFM previously in the so-called colloid probe mode [48]. Electrostatic [48], steric [49], hydrophobic [50, 51], capillary [52], hydrodynamic [53] interactions, and more, have been measured. These studies have mainly focused on nondeformable surfaces, although in recent times research on deformable systems, such as soft latex particles [54, 52], bubbles [55–57], liquid drops [58, 59], and ice [60, 61], have been reported. The experiments on microcapsule mechanics significantly extended the area of applicability of the AFM technique.

The advantage of the AFM technique is its accuracy, the possibility of studying a wider range of systems, and the richer experimental information yield: this allows one to distinguish between different regimes in load–deformation profiles, and study the permeability, elasticity, and plasticity of the capsule shell.

Up to now, all reported force versus deformation curves were measured with molecular force probe (MFP) AFM (Asylum Co., Santa Barbara, USA); the systems were equipped with a nanopositioning sensor that corrects piezoceramic hysteresis and creep. In all the experiments the MFP was used together with an inverted microscope.

A schematic diagram of the AFM experiment is presented in figure 5. This was first suggested and described in detail in [24]. Briefly, a drop of water suspension of polyelectrolyte microcapsules is deposited onto a thin glass slide fixed over the oil immersion objective of the inverted microscope. The glass sphere (radius r_s of a few tens of micrometres) is attached to a V-shaped cantilever and is centred above the apex of a capsule. The change in the separation between the glass surfaces is achieved by displacement of a piezotranslator. The typical speed of such displacement varies in the range from 0.2 to 20 μm s^{-1}, which reflects the current

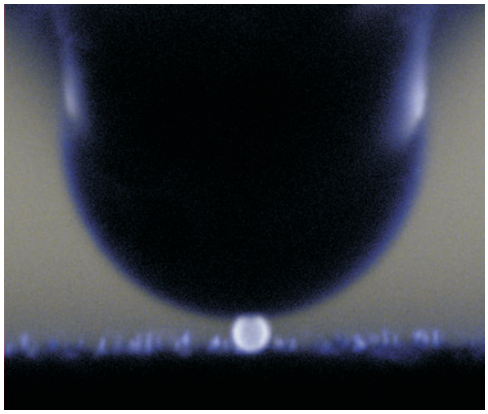

Figure 6. A confocal image of a capsule compressed between a sphere and a plane in an AFM force experiment. Reprinted with permission from [42]. Copyright (2004) American Chemical Society.

possibilities of the AFM technique and is chosen with the aim of avoiding the hydrodynamic drag on the cantilever [53, 62]. The important experimental detail is that the maximum range of displacement of an MFP piezotranslator in the vertical direction is ∼12–15 μm. This means that only capsules of $r_0 \leqslant 6$–7 μm can be deformed entirely in the AFM compression experiment.

The results of measurements represent the deflection Δ versus the position of the piezotranslator in a single approach (loading). The load, $\mathcal{F}$, was determined from the cantilever deflection, $\mathcal{F} = k\Delta$. It was suggested that the zero of separation be assumed to be at the point of the first measurable force [24]. Then the deformation is calculated as the difference between the position of the piezotranslator and the cantilever deflection.

Within the first year following the publication of the first paper on the subject [24], which employed a simple illumination scheme, the progress as regards the optical part of the set-ups included (in chronological order): fluorescence microscopy [25], reflection interference contrast microscopy (RICM) [26], confocal microscopy [17], and a special confocal scheme, which allows one to perform confocal scanning of deformed capsules both in vertical (figure 6) and horizontal directions [42].

The latter development [17, 42] deserves further comment. To our knowledge, this is the first (and only) reported combination of AFM and confocal microscopy, which represents a major step forward. The advantages of this type of optical signal combined with AFM can be summarized as follows:

- Simultaneity of optical measurements of the capsule shape during the compression.
- The possibility of working with very small capsules (r_0 of the order of micrometres). Capsules of such a size would remain invisible to conventional light microscopy. They also could not be studied with the interference technique [26] due to the low lateral resolution of the latter.
- Measurements of the volume of the compressed capsules and the permeability of the shell are made during the compression experiment.

Recent extension of this method to studying 'filled' capsules allowed us in addition to monitor the distribution of the inner polyelectrolyte under compression [72].

With an AFM method, the diameters of the capsules can be determined optically and from the load versus deformation curves (see [24] for more details). The relative deformation ε of the capsule was then defined as $\varepsilon = 1 - H/(2r_0)$ (see figure 7), where H is the separation between glass surfaces.

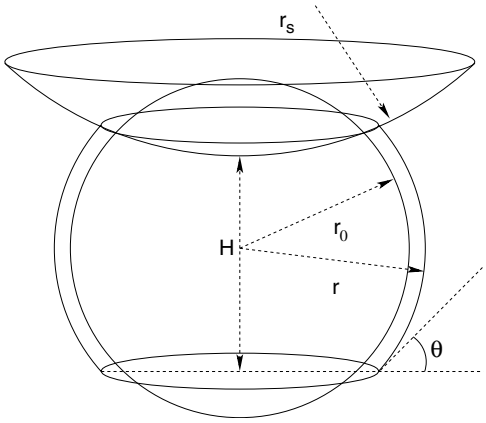

Figure 7. A sketch of the microcapsule: undeformed and deformed states. If the volume of the deformed capsule remains constant (no water drainage through the capsule shell), then the increase in the capsule radius is quadratic in the relative deformation $\varepsilon = 1 - H/(2r_0)$ (see equation (14)). Adapted from [17].

4. Theoretical review

There has been some debate about the models for fitting the experiments on the capsule mechanics. Several theories for all three methods have been explored in detail.

The main purpose of the theoretical modelling is to deduce from experiment the constants (e.g., Young's modulus, Poisson's ratio, plastic modulus) of the constitutive equations (relationship between stress and strain). These constants can then be interpreted in terms of multilayer structure and state. The second aim is to explore the influence of permeability of the shell on the mechanical behaviour of the capsules. Since the system is new, and the constitutive equation was not known *a priori*, all the suggested theories assumed the simplest linear constitutive relationship.

The main disagreement as regards the assumptions of the models concerns permeability issues. Some models ignore the finite permeability of the multilayer shells to water [27, 26]. Others distinguish between the situations of different timescales and take into account the size of the nanopores of the multilayer shell. In other words, in the situation when large pores are not formed the shell is treated as impermeable to water on short timescales [17], but as permeable on large timescales [23]. In contrast, the shells containing large pores are always treated as permeable. Below, we present the arguments and discuss the assumptions of different models. We will only mention the models developed especially for considering multilayer capsule experiments [17, 22, 23]. The models developed previously for different kinds of experiments and systems, but used to fit the capsule deformation data (e.g. [66]), are not reviewed in this section, but are briefly discussed later together with the experimental results.

4.1. Osmotically induced buckling of capsules

In the model [22] describing the shape transition from spherical to cup-like it is assumed that:

- The capsules lose their stability when the work performed by external pressure is equal to the deformation energy.
- The capsules change shape without stretching.

- The permeability of capsules to water is infinite.
- The counter-ions do not enter the capsule interior.

Strictly speaking, all the assumptions represent oversimplifications, although they could definitely be used to make rough estimates. The primitive theory of the buckling transition [22] led to a simple formula:

$$E = \frac{3P_c}{4}\left(\frac{r_0}{h}\right)^2, \tag{1}$$

where P_c is the pressure of a buckling transition.

4.2. Osmotically induced swelling of capsules

4.2.1. Work of osmotic pressure. For a dilute solution of the inner polyelectrolyte the osmotic pressure induced by the counter-ions reads

$$P = \left(\frac{r_0}{r}\right)^3 \varphi c R T. \tag{2}$$

Here c is the concentration of the polymer solution in the capsule before it swells, R is the universal gas constant, and $\varphi \leqslant 1$ is the osmotic coefficient. For bulk systems it is defined as the ratio of experimentally measured osmotic pressure P to the ideal osmotic pressure of all counter-ions. The difference between these two values is due to a fraction of condensed counter-ions being bound to the polyelectrolyte chain and not contributing to the osmotic pressure [63–65].

The work done by the osmotic pressure P in swelling the capsule from radius r_0 to r then reads

$$A = \int_{V_0}^{V} P \,\mathrm{d}V = -4\pi\varphi c R T r_0^3 T \ln\frac{r}{r_0}. \tag{3}$$

4.2.2. Elastic energy. The elastic energy of the stretching of the membrane reads [67]

$$G_s = \frac{h}{2}\int u_{\alpha\beta}\sigma_{\alpha\beta}\,\mathrm{d}S, \tag{4}$$

where h is the shell thickness ($h \ll r_0$) and the Einstein summation convention is implied, integration is over the membrane's surface, $u_{\alpha\beta}$ is the two-dimensional deformation tensor, and $\sigma_{\alpha\beta}$ is the two-dimensional stress tensor

$$\sigma_{\alpha\beta} = \frac{E}{1-\nu^2}\left[(1-\nu)u_{\alpha\beta} + \nu\delta_{\alpha\beta}u_{\gamma\gamma}\right], \tag{5}$$

where E is Young's modulus, and ν is Poisson's ratio, and summation over repeated indices is assumed.

The balance of stresses is connected with the pressure P inside the capsule by

$$\frac{h}{r}\left(\sigma_{\theta\theta} + \sigma_{\phi\phi}\right) = P. \tag{6}$$

Using the relations between the stress and deformation tensors

$$Eu_{\theta\theta} = \sigma_{\theta\theta} - \nu\sigma_{\phi\phi}, \tag{7}$$

$$Eu_{\phi\phi} = \sigma_{\phi\phi} - \nu\sigma_{\theta\theta}, \tag{8}$$

as well as

$$u_{\theta\theta} = u_{\phi\phi} = \frac{u_r}{r} = \frac{r - r_0}{r}, \tag{9}$$

one can obtain

$$\sigma_{\theta\theta} = \sigma_{\phi\phi} = \frac{E}{1-\nu}\frac{r-r_0}{r}. \tag{10}$$

Substituting equations (9), (10) into equation (4) one can derive the expression for the elastic energy due to the capsule stretching/swelling [17]:

$$G_s \approx 4\pi\frac{E}{1-\nu}h(r-r_0)^2. \tag{11}$$

4.2.3. The equilibrium radius of the swollen capsule. The equilibrium radius of the capsule is given by the minimum of the total energy $F = G + A$, where $\partial F/\partial r = 0$, giving [23]

$$r = \frac{1}{2}r_0\left(1+\sqrt{1+\frac{2\pi r_0}{h}\frac{1-\nu}{E}\varphi cRT}\right). \tag{12}$$

An important point to note is that the balance of stresses (6) gives

$$\frac{E}{1-\nu} = \frac{P}{2}\frac{r^2}{h(r-r_0)}. \tag{13}$$

Taking into account the expression for the osmotic pressure (2) one can obtain the same result (12) as in the free energy approach.

Equation (12) relates the size of the swollen capsule to the concentration of the inner solution, the thickness of the capsule shell, and Young's modulus.

This method probably gives an upper possible value of Young's modulus, because the excess osmotic pressure could be smaller than estimated from the known concentration of polyelectrolyte chains due to leaking out of counter-ions. This effect (also ignored in [22]) will effectively lead to smaller values of the Young's modulus.

It has to be stressed also that the crucial assumption of this method is that the capsule deformations are elastic. This assumption is also present in the theory of buckling [22] and other models [17], and is correct only if deformation is completely reversible. Clearly, at relatively large deformations stretching of the multilayers might be only partially reversible. Then the theoretical model describing swelling should be accommodated to the case of plastic deformations. In particular, this shows that the presence of plastic deformations would lead to underestimation of Young's modulus.

4.3. AFM force versus deformation curves

To our knowledge, there have been no theories describing a compression of 'filled' capsules in the AFM experiment. However, two simple models were used to fit the experimental data for 'hollow' capsules. Since it is more difficult to give a theoretical description of the AFM compression experiment than to give one for the other two methods, more simplifications should be involved in constructing simple analytical solutions.

4.3.1. Conservation of volume. The first model neglects drainage of the water through the capsule shell and assumes that the volume of the capsule does not change on the short timescale of the AFM experiment.

To relate the relative deformation ε and the change in the capsule radius, it was further assumed that the shape of the capsule remains spherical except in the contact regions [68] (see figure 7). Then, volume conservation requires

$$r^2 = \frac{1}{3}r_0^2\left[\frac{2+(1-\varepsilon)^3}{1-\varepsilon}\right].$$

For small ε this expression can be transformed to

$$r = r_0\left(1 + \frac{\varepsilon^2}{2}\right) + \mathcal{O}(\varepsilon^3), \tag{14}$$

where r is the final radius of the capsule. Equation (14) shows that the increase in the capsule radius is quadratic in the relative deformation ε.

If capsule deformations are small and reversible, one can use the equation (11) to find the restoring force:

$$\mathcal{F}_s = -\frac{\partial G_s}{\partial H} = 2\pi\frac{E}{1-\nu}hr_0\varepsilon^3, \tag{15}$$

which has cubic dependence on the relative deformation ε. This equation is derived for small microcapsules, i.e. when $r_0/r_s \ll 1$. A solution for capsules of arbitrary size is given in [17]. The alternative (and equivalent) way to obtain the reaction force is to multiply the pressure P from equation (6) by the microcapsule–glass sphere contact area.

The above description ignored the contribution to the elastic energy due to shell bending. This is reasonable, for a very thin shell, everywhere except at the edge of the contact area. An exact treatment of bending effects is rather complicated; the bending moment could perturb the spherical shape of the membrane near a contact, etc. However, simple estimates of the bending energy can be made. The change in curvature between the free and contact areas of the shell (a contact angle θ) occurs over a length comparable to the shell thickness, h. Then the local radius of curvature of the shell at the edge of a contact area is of the order of $\rho \approx h/\theta$ [67, 69]. The elastic energy of bending, G_b, can then be estimated from the beam theory [17, 69]:

$$G_b \approx \frac{Eh^3}{24}\frac{hl}{\rho^2}, \tag{16}$$

where $l = 4\pi r\sin\theta \approx 4\pi r\theta$ is the total length of the line separating the capsule, glass, and substrate. Substituting this back into the expression for the bending free energy (16) and taking into account that the contact area is flat, $\theta \sim \sqrt{2\varepsilon}$, one obtains [17]

$$G_b \approx \frac{\sqrt{2}\pi}{3}Eh^2r_0\varepsilon^{3/2}. \tag{17}$$

The reaction force due to shell bending reads

$$\mathcal{F}_b = -\frac{\partial G_b}{\partial H} = \frac{\pi}{2\sqrt{2}}Eh^2\varepsilon^{1/2}. \tag{18}$$

The total reaction force (load) for $r_s \gg r_0$ and $\nu = 1/2$ (the typical value for elastomer materials [68]) reads

$$\mathcal{F} = \frac{\pi}{2\sqrt{2}}Eh^2\varepsilon^{1/2} + 4\pi Ehr_0\varepsilon^3. \tag{19}$$

Comparing the reaction forces due to stretching and bending, $\mathcal{F}_s/\mathcal{F}_b \sim 8\sqrt{2}\times(r_0/h)\times\varepsilon^{5/2}$, one can conclude that as ε decreases, bending effects become more important. Also, a very thin (as compared with r_0) shell reduces the relative importance of bending. For typical experimental values, $h = 20$ nm, $r_0 = 2\ \mu$m, bending is negligibly small for relative deformations $\varepsilon \geqslant 0.15$. In contrast, stretching can safely be ignored at $\varepsilon \leqslant 0.04$.[1]

[1] Some misleading ideas about the force–deformation relationship for impermeable 'hollow' capsules may have been obtained by casual readers of the recent publication [71]. These authors omitted the bending term of equation (19) (given in [49] of their paper), and modified the stretching term, by introducing a scaling coefficient which differs from the exact one by a factor of 4/3. Since they discuss the range of deformations $\varepsilon \leqslant 0.02$, where only bending counts, such a modification of equation (19) is not justified. It led to a number of erroneous statements.

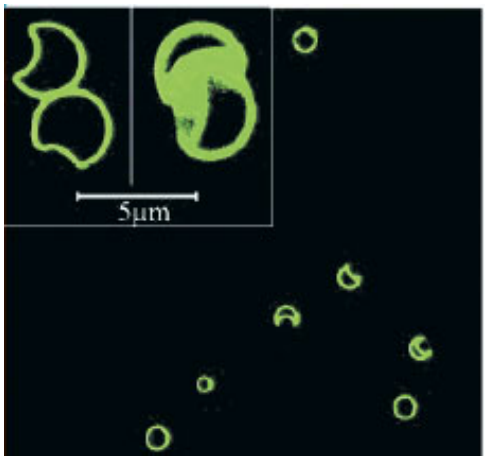

Figure 8. The buckling of 'hollow' microcapsules immersed in a PSS solution. Adapted from [22].

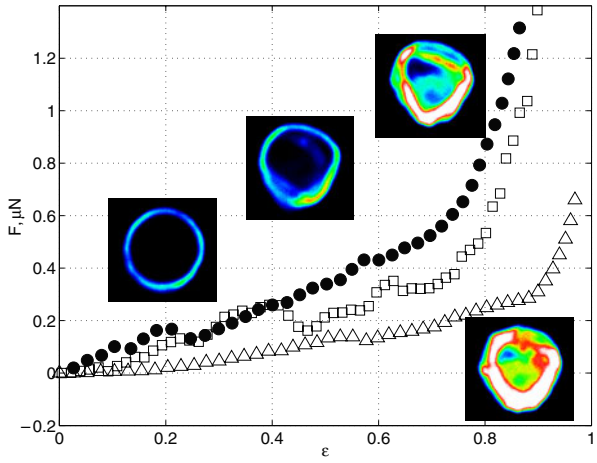

Figure 9. Typical force versus relative deformation curves and confocal images obtained at different stages of microcapsule deformation. The capsules were assembled on MF (●), $MnCO_3$ (□), and PLA (△) templates of radius $r_0 \approx 2\ \mu$m. The driving speed $v = 2\ \mu\text{m s}^{-1}$.

4.3.2. Infinite permeability. The simplified equation for this situation can be obtained similarly to the derivation of equation (18). However, if instead of flat contact condition the assumption that the curvature of the buckling zone is $-1/r_0$ is used, one can derive

$$\mathcal{F} = \sqrt{2}\pi E h^2 \varepsilon^{1/2}. \tag{20}$$

For a rough estimate, equation (18) can also be used [42].

Of course, this approach to bending is too rough an approximation, and the expressions (18) and (20) should be treated more like scaling relationships valid within the accuracy of an arbitrary coefficient. However, these estimates provide us with some guidance.

4.4. Summary

Following the analysis of several theoretical models describing various experimental situations, we suggest that all of them represent crude analytical solutions and are based on a number

of assumptions. Therefore, they might slightly underestimate or overestimate the real value of Young's modulus. Such accuracy should, however, often be enough for one to make a judgment about the physical state of the multilayer films.

5. Results and discussion; 'hollow' capsules

5.1. Osmotic buckling studies

It has to be stressed that this method [22] is a statistical one. Instead of a sharp transition point, there is a large concentration region, where the buckling starts. This is seen in figure 8, where some capsules exhibited a buckling transition, while others remained spherical. Of course, to a large extent this is connected with some variability in properties of microcapsules and other experimental factors, such as a limited resolution of optical methods. However, even with ideal experimental systems such a variability would be observed, which represents the nature of all 'phase transition' phenomena [86]. In the original publication [22], for evaluation of the value of E it was suggested that one take a concentration where 50% of the capsules are deformed. Although this 'deformation mid-point' is determined with the accuracy of 10%, such a choice of the critical pressure of buckling is arbitrary, so the error of determination of E is much larger. Therefore, this method is very approximate. This remark concerns only the value of P_c, which is probably overestimated, and a coefficient in equation (1), but not the scaling dependence itself (which seems to be the only possible one in the case where stretching can indeed be ignored).

The values of Young's modulus obtained in [22] were $E \approx 1000$–1500 MPa. Therefore, the conclusion from the osmotic buckling experiment is that polyelectrolyte multilayers represent quite a rigid material, comparable to a *bulk plastic*.

5.2. The AFM experiment

5.2.1. Regimes of deformations. The main experimental observations for capsules immersed in water were reported in [17, 24, 25]. Below we give a brief summary of these and other experimental results.

The 'hollow' capsules were found to be characterized by variability in their behaviour. Despite that, there have been some peculiarities in their deformation profiles, which always included three regimes (figure 9).

In the *first regime* with low applied load (up to $\varepsilon \leqslant 0.2$–$0.3$), the capsule deformation is elastic. Figure 9 shows profiles typical for MF capsule (loading/unloading) deformation for small relative deformations ($\varepsilon \leqslant 0.2$–$0.3$). By analysing these profiles and images from confocal scanning it was found that [17, 24]:

- The deformation is completely reversible. In other words, the capsule always returns to its original state (the force vanishes at zero deformation) during subsequent loading/unloading cycles. No deviation of the free area of the capsules from the spherical shape was found within the accuracy of the confocal measurements (figure 9).
- The pull-off force is equal to zero.
- The load–deformation profiles do not depend on the driving speed.
- The loading/unloading has hysteresis; i.e. the force upon retraction is less than that on approach at the same relative deformation (figure 10). The hysteresis is, however, relatively small.

The *second regime* of deformation corresponds to $\varepsilon \geqslant 0.2$–$0.3$. Here large hysteresis, only partial reversibility in loading/unloading, noisy regions in the deformation profiles, and

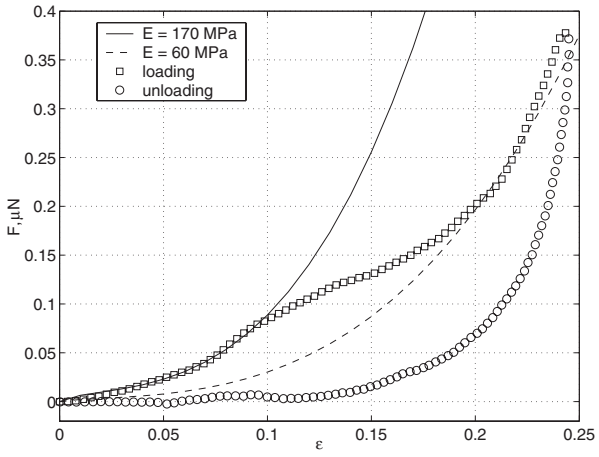

Figure 10. Typical loading (□)/unloading (○) curves for MF capsules (radius $r_0 = 2\ \mu$m). The driving speed $v = 20\ \mu\text{m s}^{-1}$. The fit to equation (19) gives an estimate for the Young's modulus in the range $E \approx 60$–170 MPa. Adapted from [17].

significant dependence on the driving speed were observed, which indicates drainage of the inner solution through the shell and/or its local ruptures. This is also confirmed by a confocal 3D scanning (figure 9).

After substantial deformation the capsules enter the *third region* ($\varepsilon \geqslant 0.7$–$0.9$), in which major damage is caused by higher load. This region is characterized by an abrupt break in the load–deformation curve and practically zero reversibility. This, together with the images of confocal scanning (figure 9), suggests total destruction of the capsules.

Of course, this subdivision is more than conventional, but it is useful for analysis of experimental results.

The comparison of force versus relative deformation curves for capsules assembled on different templates suggested that the MF and $MnCO_3$ capsules have roughly the same stiffness [21]. PLA capsules have, however, been found to be much softer (weaker force at the same ε), with much smaller hysteresis; i.e. the loading branch of the force was much closer to the unloading one [17].

The AFM experiment [24] was repeated in [26], where the optical scheme of [25] was used. The authors, however, have measured forces only at a very small deformation $\varepsilon \leqslant 0.02$, so direct comparison of their data with other publications on the subject [17, 21, 24, 25, 42], which covered much larger ranges of ε, is impossible. It is, however, clear that the authors of [26] report much larger forces at the same relative deformation, so their (PS) capsules are very stiff ($\mathcal{F} \sim 0.1\ \mu$N corresponds to $\varepsilon \sim 0.1$ for MF capsules (see figure 10) and to $\varepsilon \sim 0.02$ for PS capsules in [26]). This is probably because the preparation of PS capsules includes the treatment of the THF solution for several hours [18]. This can significantly change the shell properties.

5.2.2. The effect of the characteristic size of the capsules on their stiffness; Young's modulus in water. Since the experiment suggested that at low applied load, deformations of the capsule shells are elastic, one can fit experimental results to the prediction of models that relate the force, deformation, elastic moduli, and characteristic size of the capsules.

Which model should be chosen? Since, for capsules immersed in water, the hysteresis was found to be small and the force–deformation profiles do not depend on the driving speed

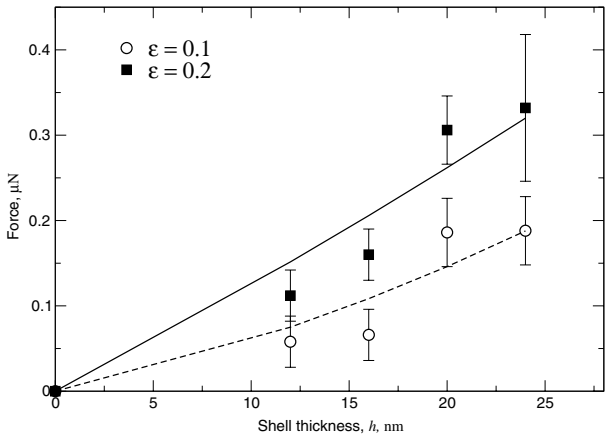

Figure 11. Load versus shell thickness for MF capsules of $r_0 = 2$ μm at relative deformations $\varepsilon = 0.1$ (○) and $\varepsilon = 0.2$ (■). The fit to equation (19) gives $E \approx 60$ MPa for $\varepsilon = 0.2$, and $E \approx 180$ MPa for $\varepsilon = 0.1$. Measurements were performed at the driving speed 20 μm s^{-1}. Reprinted with permission from [17]. Copyright (2004) American Institute of Physics.

(in the interval used), it was suggested [17] that one can, in the first approximation, neglect the drainage of water through the shell and assume that the volume of the capsule does not change on the short timescale of the AFM experiment. This situation is described by a model of capsule deformation given by equation (19). The experimental verification of this equation was carried out in [17], where the effect of the capsule radius and shell thickness on the capsule stiffness for the shells assembled on different templates was reported.

The load–deformation profiles for MF capsules were fitted to equation (19) taking the Young's modulus, E, as a fitting parameter. The fitting curves are included in figure 10. The value $E = 170$ MPa was obtained from fitting the portion of the profiles corresponding to $\varepsilon \leqslant 0.1$. The theoretical curve, which coincides with the experimental value at $\varepsilon = 0.2$, is also given and corresponds to $E = 60$ MPa. Comparison of the experimental data and theory suggests that $\varepsilon = 0.1$ is probably the limit of validity of the assumptions of the volume conservation model [17]. Clearly, the rate of drainage can become significant with further compression due to nonlinear increase in the internal pressure.

The load at a fixed relative deformation for MF capsules with different shell thicknesses h is presented in figure 11. Analysis of these data suggests that the capsules get stiffer with increase in the shell thickness, and that the effect of the shell thickness depends on the relative deformation: the crossover between $\mathcal{F} \propto h^2$ at very small ε (bending) and $\mathcal{F} \propto h$ (stretching) at larger ε is clearly seen in figure 11. The former scaling dependence for $\varepsilon \leqslant 0.02$ was also confirmed in [26] for PS capsules. Again, the volume conservation model seems to be reasonably good at $\varepsilon \leqslant 0.1$.

Thus, for MF capsules, prepared in acid media without adding any solvent or organic acid, a Young's modulus of the shell of the order of 200 MPa was obtained. The experimental dependence of the load on the shell thickness confirms that bending is important only at very low ε. The analysis of earlier data for MF capsules of the same chemical composition but prepared by dissolution of a template in more aggressive acid media [24, 25] gives a Young's modulus of the order of 30 MPa, and an even smaller value for the same capsules after treatment in organic solvent (water/acetone mixture) [25].

The volume conservation model also predicts the dependence of the reaction force on the capsule radius, given by the prefactor in equation (15) which depends on r_0. The effect

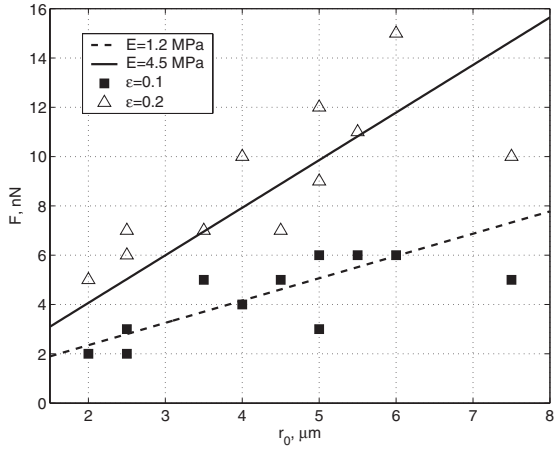

Figure 12. The force at fixed relative deformations, $\varepsilon = 0.1$ (■) and $\varepsilon = 0.2$ (△), as a function of the PLA capsule radius measured at the driving speed $v = 2\ \mu\text{m s}^{-1}$. The fit to equation (19) gives the Young's modulus $E = 4.5$ MPa (- - - -) for $\varepsilon = 0.1$ and $E = 1.2$ MPa (——) for $\varepsilon = 0.2$.

of the capsule radius was studied with the PLA capsules. Analysis of the load–deformation curves showed that bigger capsules are stiffer than smaller ones, which is consistent with the predictions of equation (19). Figure 12 shows the force at a fixed relative deformation as a function of the capsule radius. The predictions of the model are indeed confirmed by the experiment, as shown in figure 12. The important point to note is that the slope of the $\mathcal{F}$ versus r_0 straight lines gets smaller with decrease in ε, which reflects the increase in the bending contribution at very small deformations. The PLA capsules are one or two orders of magnitude softer than MF and $MnCO_3$ capsules [21, 24]. This is probably due to the organic solvent and different (and more concentrated) acid used for dissolution of the PLA templates.

Values of Young's modulus an order of magnitude larger were reported in [26] for PS capsules. As discussed above, according to the data presented these capsules are very stiff, which could be connected with the treatment with THF. Another reason could be the use of different polycations. However, before final conclusions about the values of the Young's modulus obtained in [26] are drawn, we suggest looking at the data and model, and sound a note of caution here. This concerns an obvious discrepancy between the experimental data, the theoretical model used, and the Young's modulus reported. Since this issue is very important, it makes sense to discuss it in more detail. As an experimental proof for a linear dependence of the force on ε the authors use the $\mathcal{F}$ versus ε data at $\varepsilon \leqslant 0.01$ (figures 4 and 6 of [26]). On the basis of this observation, they suggest using the theory of membrane deformation caused by a local force [66, 67]. Indeed, in some situations this scaling theory predicts $\mathcal{F} \propto Eh^2\varepsilon$. However, according to [66, 67], besides a point contact ($r_s \to 0$), which is not realistic in the case of compression by a large sphere ($r_s \gg r_0$), such a linear dependence was predicted for deformations less than the shell thickness h. With typical experimental parameters of [26] this corresponds to a ε of the order of 10^{-3}. So, great care should be taken before applying this formula to fit the AFM data. Instead, it has been shown [66, 67] that at larger ε, buckling takes place and gives $\mathcal{F} \propto Eh^2(h/r_0)^{1/2}\varepsilon^{1/2}$ (cf equation (20)). Indeed, the dependence of force on r_0 obtained in [26] in no way validates their theoretical model. It does, however, confirm a feature of the analysis published in [17]: that at very small deformations the force scales with $\sqrt{\varepsilon}$. In order to explore this more closely, the slopes of the straight lines which correspond to their $\mathcal{F}$ versus ε data and to the $\mathcal{F}/\varepsilon$ versus h^2 plot used to calculate E (figure 8 of [26]) were

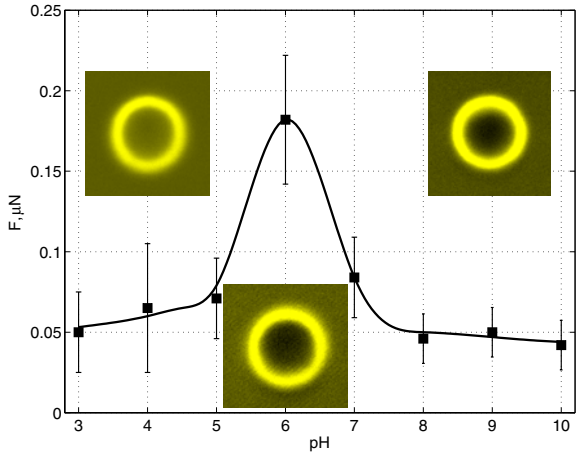

Figure 13. The force at a fixed relative deformation, $\varepsilon = 0.2$, as a function of the pH for MF capsules. The driving speed $v = 2\ \mu\text{m s}^{-1}$. Adapted from [42].

compared. It then became evident that these two sets of data differ by a factor of the order of ten[2]. If the original force versus deformation curves are correct, then the Young's modulus calculated with model [26] should be an order of magnitude larger even than that reported. In other words, it follows from the data and model presented in [26] that $E \geqslant 10^4$ MPa. These values are well above the elasticities of bulk plastics [70] and do not seem to be realistic for polyelectrolyte multilayers in water. These paradoxes should certainly be clarified.

An important conclusion from the AFM force experiment is, therefore, that the Young's modulus of polyelectrolyte multilayers falls into a range typical for *elastomer* materials [70]. The typical mechanical behaviour for elastomers reflects strong interactions between polyanions and polycations in the multilayer, and indicates that we are dealing with a physically cross-linked network structure. One reason for such a cross-link might be connected with the attraction between hydrophobic fragments of the PSS. This, in turn, could be partly responsible for the sensitivity to the organic solvent treatment. Also, the high number of ionic pairs present in the multilayers [73, 74] might serve as the cross-linking units of such a network.

5.2.3. The influence of pH and salt concentration. If the hypothesis of ionic cross-links is correct, the salt concentration could be an important physico-chemical parameter which will regulate the strength of ionic bonding and, therefore, affect the state of the multilayer and its mechanical properties. Besides that, if at least one polyelectrolyte in the multilayer is weak, the pH can be used to control the ionic cross-link density and conformations, and, therefore, should affect the stiffness of the capsules and Young's modulus of multilayer films. Despite many publications where these parameters were explored as factors controlling the multilayer growth [3, 75, 76], stability [77], permeability [78], and pore formations [79], the effect of the salt concentration and pH on the stiffness of multilayer microcapsules has been studied only recently [42].

The load at a fixed relative deformation for MF capsules with PSS/PAH shells measured in neutral, acidic, and alkaline solutions is shown in figure 13. Both decrease and increase in the pH value lead to dramatic softening of the capsules. It has been demonstrated that the reasons

[2] The slope of the original force versus deformation profiles is roughly 0.33 N m^{-1} in figure 4 of [26], and 1 N m^{-1} in their figure 6. Both force curves were obtained for $r_0 = 10\ \mu$m capsules, but in the first case the shell consisted of 10 layers, while in the second it consisted of 16 layers of alternating polyelectrolytes. However, it follows from figure 8 of [26] that the force curves for capsules of this size and with these two shell thicknesses have given slopes of ∼0.05 and ∼0.15, respectively.

for such a softening at low and high pH are different. In the former case, this is caused by the enhanced permeability of the multilayer (probably the formation of larger pores), allowing the inner solution to easily drain out even on the short timescale of the AFM force experiment. This has been proven by performing a shell permeability test for a fluorescently labelled PSS solution as a function of the pH. The corresponding confocal images are included in figure 13 and show that there is a fluorescent intensity coming from the capsule interior at low pH. Fitting to equation (20) suggests that despite the softening of the capsule, the Young's modulus remains the same as at the neutral pH. In the latter case, the capsules remain impermeable and their softening is shown to be due to weakening of the ionic cross-links. Fitting to equation (19) shows that at high pH the Young's modulus gets much smaller than in water, which probably occurs because of the decrease in the charge density of PAH.

These results unambiguously demonstrated that the elasticity of the shell and its permeability can both contribute to the 'hollow' capsule stiffness. Therefore, depending on physico-chemical conditions, different situations are possible and different models should be applied. It is also clear that in some experimental situations the intermediate situation (both drainage and stretching) could arise, which means that n in the expression $\mathcal{F} \propto \varepsilon^n$ can take values from $1/2$ to 3 (see [42]).

Results on the effect of the salt concentration on the mechanical properties of multilayer microcapsules were published in [17]. The data for PSS/PAH shells suggested that some softening of the capsules takes place. However, the measured values of forces are of the same orders of magnitude, even at 2 mol l^{-1} NaCl. This indicates that even high salt concentration does not completely dissociate polyelectrolytes in the PSS/PAH multilayers. Considerable decrease in the stiffness was, however, found later for the same PSS/PAH shells, but at higher concentrations of NaCl [80].

5.2.4. The role of molecular weight. The effect of the molecular weight of the polyelectrolyte on multilayer shells has rarely been explored. The observed effects on the assembly, structure, and thickness of supported multilayer films were extremely small [3, 73, 81, 82]. So far there has been only one attempt to estimate the influence of molecular weight on the mechanical properties of 'hollow' capsules [83]. The absence of any dependence of the force curves on the molecular weight of shell-forming polymers has been found. This result is consistent with the concept of the rubbery (elastomeric) state of the multilayer.

5.2.5. Ageing of microcapsules. The question of ageing, i.e. of the possible time evolution of the structure and properties (elasticity, permeability) of the multilayer shells, was addressed in [83]. Some softening of 'hollow' microcapsules on a relatively large (months) timescale has been detected. It has been shown that the aged capsules become softer than newly prepared ones due to the faster drainage of the inner solution under compression, which is probably caused by their enhanced fragility (or a decrease in the rupture strength). Unexpectedly, it was found that the speed of drainage from the capsules does not correlate with the tiny defect/nanopore structure of the multilayer shells. These nanopores (radii of 2–10 nm) were observed only in newly prepared capsules. They are responsible for a diffusion of macromolecules through the shells, but apparently not for drainage properties. Clearly, to better understand some variability and certain contradictions in the results of different groups as regards permeability and mechanical properties of the shells [17, 20, 22, 42, 43], these results should be taken into account.

5.3. Summary

Several additional remarks can be made to conclude this section.

- Perhaps the most promising and useful result is that the microscopic continuum mechanics approach can be applied to molecularly thin polyelectrolyte multilayer shells. In this context, an important remark would be that all the theoretical models assumed isotropic elasticity for the shell material. Their (at least qualitative) validity indicates that instead of a layered structure, we are probably dealing with a situation when layers do interpenetrate [73].
- The Young's modulus obtained in the AFM experiment is an order of magnitude lower than that obtained in the experiment on osmotically induced buckling of the same type (MF) of capsules [22]. The consequences of such differences concern mostly the physical state of the multilayer. In particular, the conclusion of [22] is that multilayers represent quite a rigid material, comparable with the *bulk plastics* [70]. In contrast to this the AFM experiments demonstrated that the value of the Young's modulus of the multilayer corresponds to that of *elastomers* [70]. Clearly, to a great extent the reasons for such a disagreement are hidden in the assumptions of the models. An order of magnitude difference cannot be treated as large, taking into account the accuracy of the experimental data and theoretical formulae, and the sensitivity of the capsule shells to the preliminary treatment and/or preparation conditions. Therefore, at the moment one cannot draw more definite conclusions about the Young's modulus value. More discriminating experiments and more critical models are needed.
- The finite permeability of the capsule shells seems to be an important factor in determining their stiffness. Therefore, a mechanical experiment can be used to study the nanopore structure of free standing multilayer films. However, it has already become clear that the diffusion and drainage permeabilities are not fully equivalent.
- The mechanical properties of the multilayer shells are extremely sensitive to the chemical treatment (e.g. the organic solvent used). Such treatments can cause changes of up to two orders of magnitude in the Young's modulus. One cannot exclude the possibility that the preparation conditions (e.g. salt concentration) might also be very important.

6. Results and discussion; 'filled' capsules

6.1. Osmotic swelling studies

After encapsulation of charged polymer molecules, the capsules swell for at least several days before reaching their equilibrium size. Therefore, all the measurements of the radius of the swollen capsules are normally performed two weeks after the filling with polyelectrolytes. Figure 14 (left) shows a typical confocal fluorescence image of the swollen capsules. The fluorescence intensity from the interior suggests a successful encapsulation. The bright interior of the capsules did not change with time, and there was no fluorescence signal from water. This proves that the capsules are impermeable for polyelectrolytes. Typical fluorescence intensity profiles across the diameter of the capsules are presented in figure 14 (right). The level of fluorescence from the wall is higher than that from the interior, which is connected with some adsorption of the inner polyelectrolyte.

Figure 15 illustrates the typical dependence of the equilibrium radius on the shell thickness. Here, the results for the $MnCO_3$ capsules filled with PSS solutions of different concentrations by a method of precipitation of complexes are given. The radius of the swollen capsules decreases with the shell thickness and is larger for the capsules with higher concentration of the inner polyelectrolyte solution. These experimental results were fitted to equation (12), taking the combination of the Young's modulus and the osmotic coefficient E/φ as a fitting

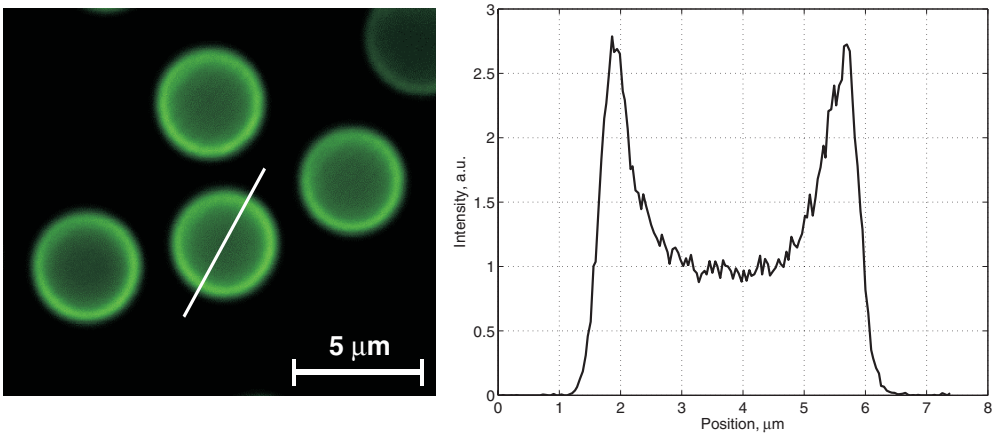

Figure 14. Confocal images of polyelectrolyte microcapsules filled with PSS (left) and a typical fluorescence profile across the diameter of the capsule (right).

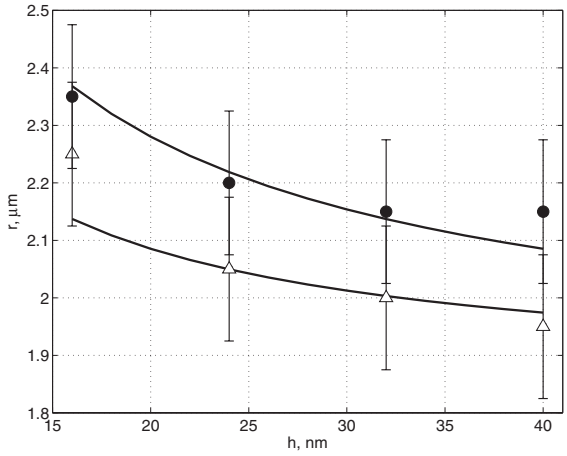

Figure 15. The radius of the swollen capsule formed on the $MnCO_3$ template of radius 1.85 μm as a function of the shell thickness. Two concentrations are shown: 0.16 mol l^{-1} (△) and 0.32 mol l^{-1} (●). The fitting (——) corresponds to $E/\varphi = 200$ MPa. (Adapted from [23].)

parameter. The value of $E/\varphi \sim 200$ MPa was obtained for both curves presented in figure 15. Thus, the predictions of the model were indeed confirmed by experiment.

The dependence of the equilibrium radius on the concentration of the inner polyelectrolyte—both the fitting curves and the experimental data—is shown in figure 16. Here data both for the $MnCO_3$ capsules formed by precipitation of complexes and for the MF capsules filled by permeability control are presented. The capsules were made on templates of different size: $r_0 = 2.5 \pm 0.2$ μm and 2.0 ± 0.1 μm, respectively. From the fit of the experimental data, $E/\varphi \sim 300$ MPa was obtained for $MnCO_3$ and $E/\varphi \sim 200$ MPa for MF capsules.

One can conclude that, taking into account realistic values of the osmotic coefficients [84, 85] for bulk PSS solutions, the Young's modulus E found in our swelling experiment is of the order of 200 MPa. This value is below the values found in the osmotic buckling experiment [22] and close to the AFM results [17, 42, 83].

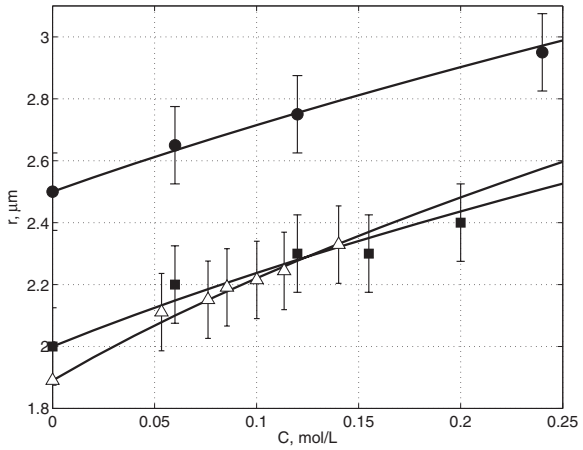

Figure 16. The radius of the swollen capsules as a function of the monomer concentration in the inner solution. Fitting (——) gave $E/\varphi = 320$ MPa ($MnCO_3$ template, ●), $E/\varphi = 180$ MPa (MF template, ■), and $E/\varphi = 110$ MPa (MF template, △).

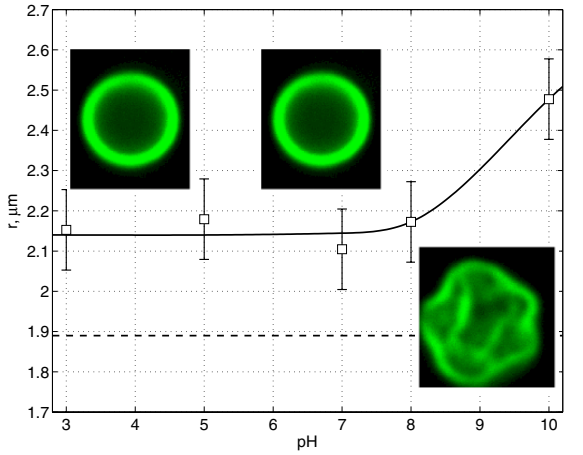

Figure 17. The equilibrium radius (□) of the PSS-filled capsules as a function of the pH and radius of the original 'hollow' capsules (- - - -). Insets show the confocal images of the capsules at the corresponding pH. Adapted from [41].

The swelling of capsules with PSS/PAH shells filled with a solution of strong polyanion was found to be pH controlled [41]. The equilibrium radius of the swollen capsules as a function of the pH is plotted in figure 17. It is seen that the capsules swollen in the high pH solution have much larger size than those immersed in low and neutral pH solutions. This indicates the softening of the multilayer shells, which is probably due to a decrease in charge density of the polycations, PAH. The capsules swollen at low pH are of the same size as those immersed in neutral pH solution, indicating the same number of ionic cross-links and the same value of Young's modulus. These observations are consistent with the results of AFM experiments with 'hollow' capsules [42]. There have been, however, some unexpected new observations differing from findings reported for 'hollow' capsules:

- It was found that the 'filled' capsules adhere strongly to the glass surface in high pH solutions.

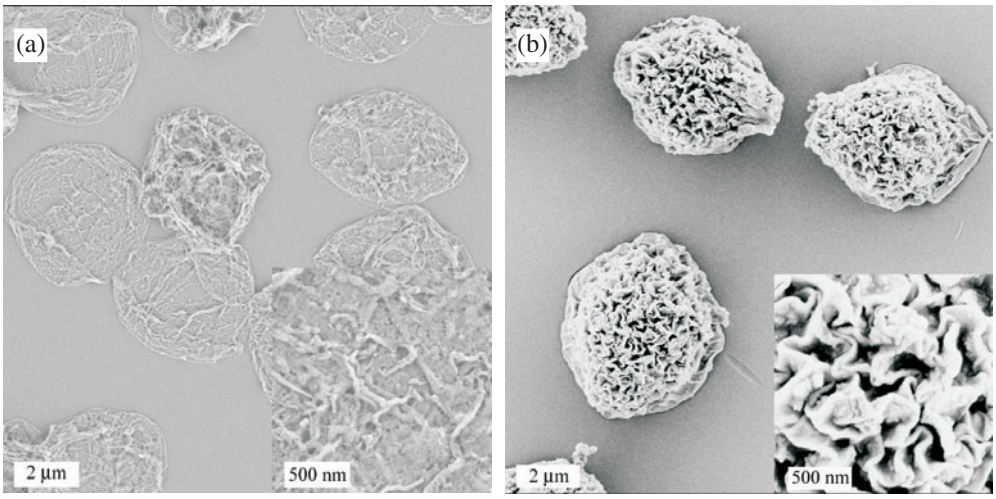

Figure 18. Scanning electron microscope images of PSS-filled $MnCO_3$ (a) and MF (b) capsules. Reprinted with permission from [21]. Copyright (2004) Wiley.

- No release of encapsulated PSS was observed in low pH solutions, although previously it was found that in these conditions the shell is permeable to PSS molecules [42]. In contrast to this, some PSS release was detected in high pH solutions, where the 'hollow' capsules were found to be in the 'closed' state. The last observation probably reflects the large degree of defect formation in the highly stretched shells.
- It should be mentioned that the study of swelling has revealed that during this process, the 'filled' capsules show an unusual significant random motion, which more or less resembles the phenomenon of Brownian motion. Moreover, it was also found that the length of the free pass of such random motion increases with the polyelectrolyte concentration. The 'filled' capsules are eventually immobilized after their equilibrium size is reached [41].

Finally, the PSS-filled capsules made on MF templates by a precipitation technique were reported to be of much larger size [24, 37] than the MF capsules made by permeability control [23, 41], and $MnCO_3$ capsules made by precipitation of a complex [21]. Assuming that the properties of the shell remain the same, this indicates a much higher osmotic pressure of the inner PSS solution. It was suggested that this might be caused by the rest of the positively charged MF oligomers inside the capsules, which increase the excess osmotic pressure and lead to the formation inside such 'filled' capsules of electrostatically stabilized hydrogel-like structures [24]. This hypothesis was confirmed in [21]. The existence of such a hydrogel in the interior of PSS-filled MF capsules made by precipitation of complexes was proved by the presence of characteristic MF bands in the confocal Raman spectra, and the bulk-like morphology of the dried capsules studied by scanning electron microscopy (figure 18). No gel-like structure was observed in other kinds of 'filled' capsules. Since the current model of microcapsule swelling does not describe the swelling of capsules filled with hydrogels, the results for these, superswollen, capsules were not analysed quantitatively.

6.2. The AFM experiment

6.2.1. Capsules filled with the neutral polymer. To our knowledge there has been only one attempt to explore the mechanical behaviour of capsules filled with a neutral polymer,

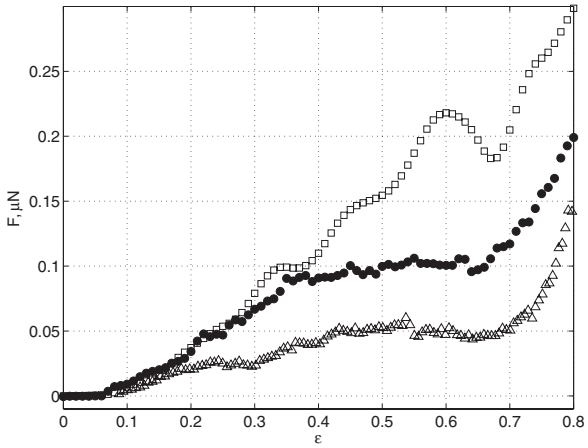

Figure 19. Force versus deformation curves for capsules filled with FITC dextran (10 g l^{-1}) measured at driving speeds of 0.2 (△), 2 (●), and 20 (□) μm s^{-1}. Adapted from [25].

dextran [25]. The essential observations were these:

- Capsules with different concentrations of dextran show qualitatively similar deformation profiles, the same as those previously observed for 'hollow' capsules [24]—that is, the deformation profiles always include three distinct regimes of deformations, characterized by different reversibilities.
- In the first, elastic regime of deformation the force does not depend on the concentration of the inner polymer, which suggests that the osmotic pressure of neutral polymer is too low to play any role. There is a contribution to the stiffness of the microcapsules from the inner polymer solution in the second regime of deformation.
- The deformation profiles are not sensitive to the driving speed at small relative deformations (first regime), but the capsule stiffness increases with the concentration of the inner polymer at larger deformation (second and third regimes) (figure 19).

Thus, a nearly absolute match to the 'hollow' capsule behaviour was found for capsules filled with a neutral polymer. The observed dependence of the force on the driving speed and concentration of the inner solution at relatively large deformation might serve as an indication of finite permeability of the capsule shell.

6.2.2. Capsules filled with the polyelectrolyte. Here the experimental information is still limited; however, three recent publications [21, 24, 72] lead us to suggest that the capsules filled with polyelectrolyte are stiffer than 'hollow' ones. Another thing to note is that there is an obvious effect of the template material and encapsulation method on the force versus deformation profiles.

Studies on the stiffness of 'filled' capsules made by precipitation of complexes have been reported in [21, 24]. The main experimental observations are the following. Qualitatively, the $MnCO_3$ capsules are similar to 'hollow' ones or ones filled with a neutral polymer, although they seem to be stiffer [21]. The MF capsules reveal qualitatively different behaviour. In this case, it was suggested that one distinguish between two regimes of deformations. As for 'hollow' capsules, the *first regime* ($\varepsilon \leqslant 0.2$–$0.3$) is characterized by low hysteresis and reversibility of deformation. Further deformation (ε up to 0.5–0.8) corresponds to the *second*

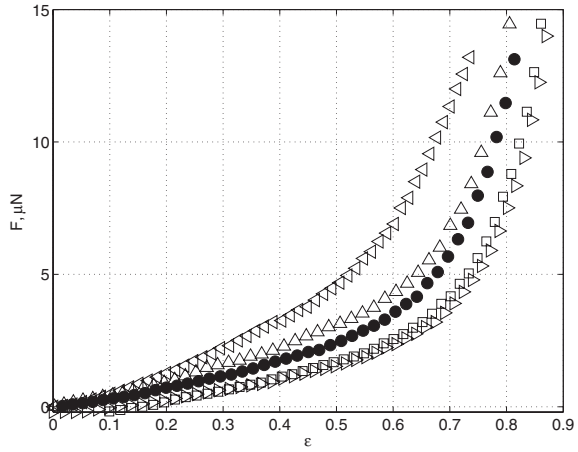

Figure 20. Force versus deformation curves for MF capsules filled with PSS by precipitation of complexes. The driving speed 0.2 μm s^{-1}. From top to bottom, the results are for capsules immersed in water and 10^{-3}, 10^{-2}, 10^{-1}, and 1 mol l^{-1} NaCl, respectively. Adapted from [24].

regime, where an increase in hysteresis and only partial reversibility with applied force are shown. In particular, the capsules do not reveal variability in behaviour, and become stiffer when the load is increased. Their rupture during the compression experiment was never observed. Thus, encapsulation of polyelectrolyte can dramatically change the mechanical properties of polyelectrolyte microcapsules.

The possible reasons for the increase in stiffness are probably connected with the excess osmotic pressure of counter-ions inside capsules. One could suggest that this effect is entirely responsible for the increased stiffness of 'filled' $MnCO_3$ capsules. The behaviour of MF capsules is more complicated. Clearly, in this case an osmotic pressure also plays some role. Indeed, the capsules get softer with increasing salt concentration [24] (see figure 20). However, even for 1 mol l^{-1} salt solution, the force versus relative deformation profiles are well above the curves obtained for 'hollow' capsules. Therefore, a single osmotic pressure mechanism cannot account for effect of salt concentration on the mechanical properties of 'filled' capsules. These experimental observations were interpreted in terms of gel-like structure inside the capsules [24] and were confirmed later [21] by confocal Raman and scanning electron microscopy. More details about other factors leading to 'filled' capsule stiffness can be found in the original paper [24].

The results obtained for capsules filled with the same polyelectrolyte solution, but by different (permeability control) techniques, have been reported in [72]. The MF capsules prepared by this method were found to be similar to 'hollow' ones or ones filled with a neutral polymer, although they are a few times stiffer. In other words, they have led to force–deformation curves comparable to those measured for $MnCO_3$ capsules filled by precipitation of complexes [21]. This probably reflects the contribution of osmotic pressure only to the increase in stiffness. The force–deformation curves measured for capsules with different amounts of encapsulated PSS suggested that the capsules get stiffer with increase of the inner polyelectrolyte concentration, which is consistent with the expected effect of osmotic pressure. The simultaneous confocal measurements performed in [72] allowed us to relate the (three) regimes of deformations to the permeability of the multilayer shells for water and inner polyelectrolyte at different stage of compression. Thus the analysis of the distribution of the fluorescence intensity measured at the equatorial cross-section (figure 21) allowed one

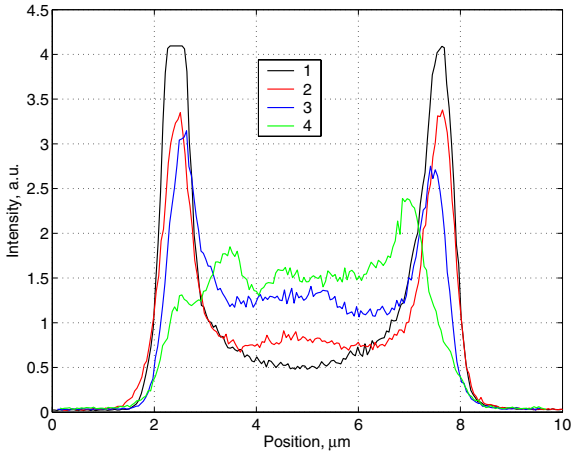

Figure 21. The intensity of the fluorescence measured along the equatorial cross-section line for compressed capsules: $\varepsilon = 0.1$ (1), 0.3 (2), 0.5 (3), and 0.7 (4). Adapted from [72].

to conclude that at small relative deformations the inner PSS concentration remains constant, confirming the constant volume assumption. At larger deformation, the concentration of inner polymer increases. This experimental fact confirms that the partial reversibility of the deformation is caused by significant water drainage.

6.3. Summary

The results described above suggest that the 'filled' capsules reveal a richer mechanical behaviour as compared with 'hollow' capsules, and that there is a complex interplay between the elastic properties of the shell, its permeability, and the structure of the inner solution. From that point of view, the 'filled' capsules represent much more interesting systems than 'hollow' ones. However, whilst the first experimental results seem to be very promising, the theoretical understanding of the mechanics of 'filled' capsules is not so advanced. For example, it has become evident already, from the intensity of the fluorescence distribution (figure 14), which shows some adsorption of the inner polyelectrolyte at the shell, that there is a contribution from the polymer itself to the excess osmotic pressure. The same feature probably indicates that the counter-ions leak out, which means that the effective osmotic coefficient is smaller than for the bulk. Neither effect is included in the model of microcapsule swelling (in fact, the same remark also applies to osmotic buckling experiments). The theory of the compression of 'filled' capsules in the AFM experiment is still lacking, although such a theory might shed some light on the value of the effective osmotic coefficient of the encapsulated solution, and other aspects of capsule mechanics.

7. Concluding remarks

In this article, we have reviewed some of the recent studies on mechanical properties of both 'hollow' and 'filled' (with charged and neutral polymer) polyelectrolyte multilayer microcapsules. Three methods of measurement—osmotic buckling [22], osmotic swelling [23], and AFM compression experiments [17, 24]—have been discussed. The theoretical background of each has been detailed, and experimental data have been critically

analysed. Since the mechanics of polyelectrolyte microcapsules is a new area of research, there remain unanswered a number of questions. Some of them are specified below.

What development can be expected? There is no doubt that mechanical studies will continue. The present methods and set-ups are very sensitive, and are good enough for making very accurate measurements of forces, deformations, shape, permeability, etc. Of course, we do not exclude the possibility of a substantial modification of the present methods or set-ups, or the appearance of a new experimental technique for studying mechanical properties of polyelectrolyte multilayer microcapsules. However, it seems more likely that the main focus of research will be shifted from the development of new methods to studying various microcapsule systems in more detail. Extensions could include, for example, more detailed investigation of 'filled' capsules and studies of adhesion properties. Since the majority of results reported so far concerned mostly PSS/PAH multilayers, other combinations of polyelectrolytes have to be explored and might lead to entirely new scenarios and/or different results. Of course, the search for more accurate models of microcapsule deformations is also necessary (although the present ones do seem to capture the essential physics). For example, further work on the investigation of the role of finite permeability of the multilayer shell might help us to improve the existing models for describing AFM experiments and to learn more about tiny and large nanopore structures of free standing multilayer films. More discriminating swelling experiments with capsules filled with high concentration polyelectrolyte solutions might lead to the possibility of plastic regimes of deformations and shed some light on such parameters of multilayers as the plastic modulus, yield stress, and tensile strength. They could also help us to understand the role of charged polymer molecules and counter-ions in determining the osmotic equilibria as factors controlling the stiffness of 'filled' capsules.

Despite these fundamental issues awaiting clarification, enough is now known about the mechanical properties of polyelectrolyte microcapsules for us to explore the practical implications. In the context of (*elastomer*) elastic properties one can now understand the extreme stability of polyelectrolyte multilayer films and their good ageing properties in various solutions. One can speculate that this long term stability of films, which do not represent equilibrium structures [77], is attributable to the same types of ionic (and perhaps other) cross-linking as that responsible for a mechanical behaviour. Such cross-links can reduce the mobility of polyelectrolyte chains, thus freezing the structure of the multilayers. The possibility of controlling mechanical properties by regulating the elasticity/permeability of the shell and adjusting the concentration of the encapsulated polymer offers a novel approach to the designing of new composite materials with well defined stiffness. This, entirely unexplored, area of materials science ought to be developed. As one possible approach to increasing the capsule stiffness, the incorporation of nanoparticles into the shell could be suggested [87, 88]. One can also expect the focus to be shifted to more bio-oriented systems than the synthetic polyelectrolytes discussed here; one could employ biopolymers (DNA, proteins) [36, 89] which represent polyelectrolytes and polyampholytes. Studying mechanical and adhesion properties of such microcapsules will allow us to mimic the behaviour of living and artificial cells in various conditions.

Acknowledgments

This review summarizes the work of many friends and colleagues, and it is my pleasure to acknowledge their contributions. This holds, in particular, for the PhD dissertation of V V Lulevich and Diploma thesis of S Nordschild. I would like to thank D Andrienko, B S Kim, O V Lebedeva, and M R Stukan, who also worked with me on the capsule project at the MPI for Polymer Research in Mainz. I am happy to mention many intellectual contributions by our

colleagues at the MPI for Colloid and Interface Research in Golm, first of all, A A Antipov, G B Sukhorukov and I L Radtchenko. The lively debates with H Möhwald and his criticism were essential to the development of a common viewpoint. Last but not least, I profited from numerous discussions with A R Khokhlov, K Kremer, H Schiessel, G Wegner, and A B Zezin. The (strategic) advice of W Knoll has always been of considerable help. Without some of this assistance, this review could not have been written. Financial support came from the Max Planck Society and the Alexander von Humboldt Foundation.

References

[1] Donath E, Sukhorukov G B, Caruso F, Davis S A and Möhwald H 1998 *Angew. Chem. Int. Edn Engl.* **37** 2202
[2] Decher G 1997 *Science* **277** 1232
[3] Bertrand P, Jonas A, Laschewsky A and Legras R 2000 *Macromol. Rapid Commun.* **21** 319
[4] Schönhoff M 2003 *J. Phys.: Condens. Matter* **15** R1781
[5] Sukhorukov G B, Donath E, Lichtenfeld H, Knippel E, Knippel M, Budde A and Möhwald H 1998 *Colloids Surf.* A **137** 253
[6] Lewis D D 1990 *Controlled Release of Bioactive Agents from Lactide/Glycolide Polymers* ed M Chasin and R Langer (New York: Dekker)
[7] Deserno M and Gelbart W M 2002 *J. Phys. Chem.* B **106** 5543
[8] Evans E A and Skalak R 1980 *Mechanics and Thermodynamics of Biomembranes* (Boca Raton, FL: CRC Press)
[9] Daily B, Elson E L and Zahalak G I 1984 *Biophys. J.* **45** 671
[10] Liu K K, Williams D R and Briscoe B J 1996 *Phys. Rev.* E **54** 6673
[11] Hochmuth R M 2000 *J. Biomech.* **33** 15
[12] Carin M, Barthès-Biesel D, Edwards-Lévy F, Postel C and Andrei D A 2003 *Biotechnol. Bioeng.* **82** 207
[13] Bäumler H, Artmann G, Voight A, Miltlöhner R, Neu B and Kiesewetter H 2000 *J. Microencapsul.* **17** 651
[14] Sukhorukov G B 2001 *Novel Methods to Study Interfacial Layers* ed D Mobius and R Millers (Amsterdam: Elsevier) p 384
[15] Gao C Y, Moya S, Lichtenfeld H, Casoli A, Fiendler H, Donath E and Möhwald H 2001 *Macromol. Mater. Eng.* **286** 355
[16] Shenoy D B, Antipov A A, Sukhorukov G B and Möhwald H 2003 *Biomacromolecules* **4** 265
[17] Lulevich V V, Andrienko D and Vinogradova O I 2004 *J. Chem. Phys.* **120** 3822
[18] Pastoriza-Santos I, Schöler B and Caruso F 2001 *Adv. Funct. Mater.* **11** 122
[19] Silvano D, Krol S, Diaspro A, Cavalleri O and Gliozzi A 2002 *Micros. Res. Tech.* **59** 536
[20] Antipov A A, Sukhorukov G B, Leporatti S, Radtchenko I L, Donath E and Möhwald H 2002 *Colloids Surf.* A **198** 535
[21] Sukhorukov G B, Shchukin D G, Dong W F, Möhwald H, Lulevich V V and Vinogradova O I 2004 *Macromol. Chem. Phys.* **205** 530
[22] Gao C, Donath E, Moya S, Dudnik V and Möhwald H 2001 *Eur. Phys. J.* E **5** 21
[23] Vinogradova O I, Andrienko D, Lulevich V V, Nordschild S and Sukhorukov G B 2004 *Macromolecules* **37** 1113
[24] Lulevich V V, Radtchenko I L, Sukhorukov G B and Vinogradova O I 2003 *J. Phys. Chem.* B **107** 2735
[25] Lulevich V V, Radtchenko I L, Sukhorukov G B and Vinogradova O I 2003 *Macromolecules* **36** 2832
[26] Dubreuil F, Elsner N and Fery A 2003 *Eur. Phys. J.* E **12** 215
[27] Gao C, Leporatti S, Moya S, Donath E and Möhwald H 2001 *Langmuir* **17** 3491
[28] Decher G and Schmitt J 1992 *Prog. Colloid Polym. Sci.* **89** 160
[29] Lvov Y, Decher G and Möhwald H 1993 *Langmuir* **9** 481
[30] Lvov Y, Decher G, Haas H, Möhwald H and Kalachev A 1994 *Physica* B **198** 89
[31] Clark S L, Montague M F and Hammond P T 1997 *Macromolecules* **30** 7237
[32] Hoogeveen N G, Cohen Stuart M A and Fleer G J 1996 *J. Colloid Interface Sci.* **182** 133
[33] Caruso F, Niikura K, Furlong D N and Okahata Y 1997 *Langmuir* **13** 3422
[34] Sukhorukov G B, Donath E, Davis S, Lichtenfeld H, Caruso F, Popov V I and Möhwald H 1998 *Polym. Adv. Technol.* **9** 759
[35] Sukhorukov G B, Antipov A A, Voigt A, Donath E and Möhwald H 2001 *Macromol. Rapid Commun.* **22** 44
[36] Lvov Y, Antipov A A, Mamedov A, Möhwald H and Sukhorukov G B 2001 *Nano Lett.* **1** 125
[37] Radtchenko I L, Sukhorukov G B, Leporatti S, Khomutov G B, Donath E and Möhwald H 2000 *J. Colloid Interface Sci.* **230** 272

[38] Radtchenko I L, Sukhorukov G B and Möhwald H 2002 *Colloids Surf.* A **202** 127
[39] Dudnik V, Sukhorukov G B, Radtchenko I L and Möhwald H 2001 *Macromolecules* **34** 2329
[40] Dähne L, Leporatti S, Donath E and Möhwald H 2001 *J. Am. Chem. Soc.* **123** 5431
[41] Kim B S and Vinogradova O I 2004 *J. Phys. Chem.* B **108** 8161
[42] Lulevich V V and Vinogradova O I 2004 *Langmuir* **20** 2874
[43] Izbarz G, Däne L, Donath E and Möhwald H 2001 *Adv. Mater.* **13** 1324
[44] Takahashi A, Kato N and Nagasawa M 1970 *J. Phys. Chem.* **74** 944
[45] Wang L and Bloomfield V A 1990 *Macromolecules* **23** 804
[46] Barrat J L and Joanny J F 1996 *Adv. Chem. Phys.* **94** 1
[47] Sukhorukov G B, Brumen M, Donath E and Möhwald H 1999 *J. Phys. Chem.* B **103** 6434
[48] Ducker W A, Senden T J and Pashley R M 1991 *Nature* **353** 239
[49] Butt H J, Kappl M, Müller H and Raiteri R 1999 *Langmuir* **15** 2559
[50] Craig V S J, Ninham B W and Pashley R M 1999 *Langmuir* **15** 1562
[51] Yakubov G E, Butt H J and Vinogradova O I 2000 *J. Phys. Chem.* B **104** 3407
[52] Vinogradova O I, Yakubov G E and Butt H J 2001 *J. Chem. Phys.* **114** 8124
[53] Vinogradova O I and Yakubov G E 2003 *Langmuir* **19** 1227
[54] Considine R F, Hayes R A and Horn R G 1999 *Langmuir* **15** 1657
[55] Ducker W A, Xu Z and Israelachvili J N 1994 *Langmuir* **10** 3279
[56] Fielden M L, Hayes R A and Ralston J 1996 *Langmuir* **12** 3721
[57] Yakubov G E, Vinogradova O I and Butt H J 2000 *J. Adhes. Sci. Technol.* **14** 1783
[58] Aston D E and Berg J C 2001 *J. Colloid Interface Sci.* **12** 461
[59] Dagastine R R, Prieve D C and White L R 2004 *J. Colloid Interface Sci.* **269** 84
[60] Butt H J, Döppenschmidt A, Hüttl G, Müller E and Vinogradova O I 2000 *J. Chem. Phys.* **113** 1194
[61] Pittenger B, Fain S C, Cochran M J, Donev J M K, Robertson B E, Szuchmacher A and Overney R M 2001 *Phys. Rev.* B **63** 134102
[62] Vinogradova O I, Butt H J, Yakubov G E and Feuillebois F 2001 *Rev. Sci. Instrum.* **72** 2330
[63] Stevens M J and Kremer K 1995 *J. Chem. Phys.* **103** 1690
[64] Micka U, Holm C and Kremer K 1999 *Langmuir* **15** 4044
[65] Liao Q, Dobrynin A V and Rubinstein M 2003 *Macromolecules* **36** 3399
[66] Helfer E, Harlepp S, Bourdieu L, Robert J, MacKintosh F C and Chatenay D 2001 *Phys. Rev. Lett.* **87** 088103
[67] Landau L D and Lifshitz E M 1995 *Theory of Elasticity* (Oxford: Butterworth-Heinemann)
[68] Shanahan M E R 1997 *J. Adhes.* **63** 15
[69] Shanahan M E R 2003 *J. Adhes.* **79** 881
[70] Shackelford J F, William A and Juns P 1992 *Material Science and Engineering Handbook* (Boca Raton, FL: CRC press)
[71] Fery A, Dubreuil F and Möhwald H 2004 *New J. Phys.* **6** 18
[72] Lebedeva O V, Kim B S and Vinogradova O I 2004 *Langmuir* submitted
[73] Lösche M, Schmitt J, Decher G, Bouwman W G and Kjaer K 1998 *Macromolecules* **31** 8893
[74] Lowack K and Helm C A 1998 *Macromolecules* **31** 823
[75] Dubas S T and Schlenoff J B 1999 *Macromolecules* **32** 8153
[76] Shiratori S and Rubner M 2000 *Macromolecules* **33** 4213
[77] Hoogeveen N G, Cohen Stuart M A and Fleer G J 1996 *Langmuir* **12** 3675
[78] Antipov A A, Sukhorukov G B and Möhwald H 2003 *Langmuir* **19** 2444
[79] Mendelsohn J D, Barret C J, Chan V V, Pal A J, Mayes A M and Rubner M 2000 *Langmuir* **16** 5017
[80] Lebedeva O V, Kim B S and Vinogradova O I 2004 *Macromolecules* submitted
[81] Kolarik L, Furlong D N, Joy H, Struijk C and Rowe R 1999 *Langmuir* **15** 8265
[82] Sui Z, Salloum D and Schlenoff J B 2003 *Langmuir* **19** 2491
[83] Lulevich V V, Nordschild S and Vinogradova O I 2004 *Macromolecules* submitted
[84] Essafi W, Lafuma F and Williams C E 1995 *J. Physique* II **5** 1267
[85] Essafi W, Lafuma F and Williams C E 1999 *Eur. Phys. J.* B **9** 261
[86] Andrienko D, Patricio P and Vinogradova O I 2004 *J. Chem. Phys.* at press
[87] Tang Z, Kotov N A, Magonov A and Ozturk B 2003 *Nat. Mater.* **9** 413
[88] Jiang C Y, Markutsya S and Tsukruk V V 2004 *Adv. Mater.* **16** 157
[89] Shchukin D G, Patel A A, Sukhorukov G B and Lvov Y M 2004 *J. Am. Chem. Soc.* **126** 3374